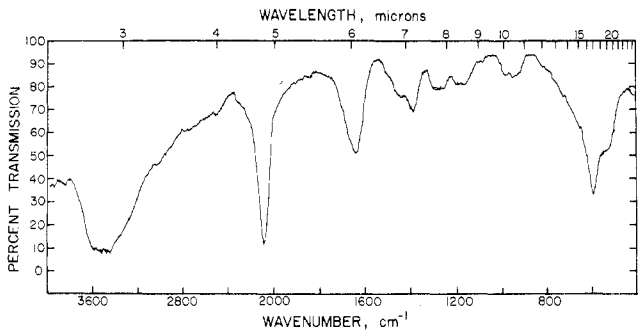

Figure 10. Infrared spectrum of $Fe(CN)_5N(O)CH_2C(CH_3)_2OH^{3-}$ in a KBr matrix.

and 1631 cm^{-1} may be assigned to lattice H_2O; the band at 3500 cm^{-1} would obscure the O–H alcohol mode expected in this region. Bands at 590 and 525 cm^{-1} are attributed to ν_{Fe-CN}.[41] Between 1575 and 1150 cm^{-1}, several weak bands are resolved which occur in regions characteristic of both the fingerprint for the alkyl backbone and ν_{NO} of the nitroso moiety.[43]

The reaction of $Fe(CN)_5NO^{3-}$ with free radicals appears

$$Fe(CN)_5NO^{3-} + R\cdot \rightarrow Fe(CN)_5N(O)R^{3-} \quad (7)$$

to be a general synthetic route to iron alkylnitroso complexes and their derivatives. Further details about reaction 7 and the analogous reaction of $Ru(NH_3)_5NO^{2+}$ will be presented in a separate publication.[44]

Registry No. $Fe(CN)_5NO^{2-}$, 15078-28-1; $Fe(CN)_5NO^{3-}$, 14636-58-9; $Fe(CN)_4NO^{2-}$, 55188-49-3; $Fe(CN)_5N(O)CH_2C(CH_3)_2OH^{3-}$, 63231-44-7; CN^-, 57-12-5.

References and Notes

(1) Research supported in part by the U.S. Army through Contract DAAG17-76-C-0009 to Boston University. Presented in part at the 173rd National Meeting of the American Chemical Society, New Orleans, La., March 1977; see Abstracts, No. INOR 131.
(2) (a) Boston University. (b) U.S. Army NRDC. (c) Hahn-Meitner Institut.
(3) M. C. R. Symons, D. X. West, and J. G. Wilkinson, *Inorg. Chem.*, **15**, 1022 (1976), and references therein.
(4) J. Schmidt and W. Dorn, *Inorg. Chim. Acta*, **16**, 223 (1976), and references therein.
(5) (a) J. Masek and E. Maslova, *Collect. Czech. Chem. Commun.*, **39**, 214 (1974), and references therein; (b) W. L. Bowden, P. Bonnar, D. B. Brown, and W. E. Geiger, Jr., *Inorg. Chem.*, **16**, 41 (1977).
(6) J. N. Armor and M. Z. Hoffman, *Inorg. Chem.*, **14**, 444 (1975).
(7) J. N. Armor, R. Furman, and M. Z. Hoffman, *J. Am. Chem. Soc.*, **97**, 1737 (1975).
(8) The system has been investigated briefly by pulse radiolysis: G. V. Buxton, F. S. Dainton, and J. Kalecinski, *Int. J. Radiat. Phys. Chem.*, **1**, 87 (1966).
(9) (a) K.-D. Asmus, *Int. J. Radiat. Phys. Chem.*, **4**, 417 (1972); (b) K.-D. Asmus in "Fast Processes in Radiation Chemistry and Biology", G. E. Adams, E. M. Fielden, and B. D. Michael, Ed., Wiley, New York, N.Y., 1973, p 40.
(10) J. Lilie and R. W. Fessenden, *J. Phys. Chem.*, **77**, 674 (1973).
(11) M. Simic and J. Lilie, *J. Am. Chem. Soc.*, **96**, 291 (1974).
(12) M. Simic, P. Neta, and E. Hayon, *J. Phys. Chem.*, **73**, 3794 (1969).
(13) J. H. Baxendale, P. L. T. Bevan, and D. A. Stott, *Trans. Faraday Soc.*, **64**, 2398 (1968).
(14) G. Beck, *Int. J. Radiat. Phys. Chem.*, **1**, 361 (1969).
(15) K.-D. Asmus, H. Möckel, and A. Henglein, *J. Phys. Chem.*, **77**, 1218 (1973).
(16) L. M. Dorfman and G. E. Adams, *Natl. Stand. Ref. Data Ser., Natl. Bur. Stand.*, **No. 46** (1973).
(17) M. Anbar, M. Bambenek, and A. B. Ross, *Natl. Stand. Ref. Data Ser., Natl. Bur. Stand.*, **No. 43** (1972).
(18) M. Anbar, Farhataziz, and A. B. Ross, *Natl. Stand. Ref. Data Ser., Natl. Bur. Stand.*, **No. 51** (1975).
(19) M. G. Simic, M. Z. Hoffman, and N. V. Brezniak, *J. Am. Chem. Soc.*, **99**, 2166 (1977).
(20) M. B. Shin, *Ind. Eng. Chem.*, **13**, 33 (1941).
(21) J. D. W. Van Voorst and P. Hemmerich, *J. Chem. Phys.*, **45**, 3914 (1967).
(22) J. H. Swinehart and P. A. Rock, *Inorg. Chem.*, **5**, 573 (1966); J. Masek and H. Wendt, *Inorg. Chim. Acta*, **3**, 455 (1969).
(23) E. J. Hart and M. Anbar, "The Hydrated Electron", Wiley-Interscience, New York, N.Y., 1970, p 118.
(24) (a) R. Nast and J. Schmidt, *Angew. Chem.*, **81**, 399 (1969); (b) J. Schmidt, H. Kuhr, W. L. Dorn, and J. Kopf, *Inorg. Nucl. Chem. Lett.*, **10**, 55 (1974); (c) R. Nast and J. Schmidt, *Z. Anorg. Allg. Chem.*, **421**, 15 (1976).
(25) J. Masek and J. Dempir, *Collect. Czech. Chem. Commun.*, **34**, 727 (1969).
(26) C. Capellos and B. H. J. Bielski, "Kinetic Systems", Wiley-Interscience, New York, N.Y., 1972.
(27) J. Jordan and G. J. Ewing, *Inorg. Chem.*, **1**, 587 (1962).
(28) J. H. Enemark, R. D. Feltham, J. Riker-Nappier, and K. F. Bizot, *Inorg. Chem.*, **14**, 624 (1975), and references therein.
(29) R. P. Cheney, M. Z. Hoffman, and J. A. Lust, in preparation.
(30) R. W. Callahan, G. M. Brown, and T. J. Meyer, *J. Am. Chem. Soc.*, **97**, 894 (1975); R. W. Callahan and T. J. Meyer, *Inorg. Chem.*, **16**, 574 (1977).
(31) P. T. Manoharan and H. B. Gray *J. Am. Chem. Soc.*, **87**, 3340 (1965).
(32) R. A. Nyquist and R. O. Kagel, "Infrared Spectra of Inorganic Compounds", Academic Press, New York, N.Y., 1971.
(33) S. Pell and J. N. Armor, *Inorg. Chem.*, **12**, 873 (1973).
(34) M. B. Fairley and R. J. Irving, *Spectrochim. Acta*, **22**, 359 (1966).
(35) E. E. Mercer, W. M. Campell, and R. M. Wallace, *Inorg. Chem.*, **3**, 1018 (1964).
(36) R. G. Wilkins, *Adv. Chem. Ser.*, **No. 100**, 111 (1971).
(37) J. Lilie, M. G. Simic, and J. F. Endicott, *Inorg. Chem.*, **14**, 2129 (1975).
(38) W. P. Griffith, *Q. Rev., Chem. Soc.*, **16**, 188 (1962).
(39) N. V. Sidgwick, "The Chemical Elements and Their Compounds", Clarendon Press, Oxford, England, 1950, p 1345.
(40) J. H. Swinehart and W. G. Schmidt, *Inorg. Chem.*, **6**, 232 (1967).
(41) L. Tosi and J. Danon, *Inorg Chem.*, **3**, 150 (1964).
(42) "Sadtler Standard IR Spectra", Sadtler Research Laboratories, Philadelphia, Pa., 1956, No. 2B.
(43) C. J. Popp and R. O. Ragsdale, *Inorg. Chem.*, **7**, 1845 (1968).
(44) R. P. Cheney, S. D. Pell, and M. Z. Hoffman, in preparation.

Contribution from the Department of Chemistry, York University, Downsview, Ontario, Canada

Kinetics and Equilibria for Carbon Monoxide and Benzyl Isocyanide Binding to Ferrous Tetrabenzo[*b*,*f*,*j*,*n*][1,5,9,13]tetraazacyclohexadecine

I. W. PANG and DENNIS V. STYNES*

Received September 7, 1976 AIC60669O

Syntheses, visible spectra, and NMR are reported for low-spin iron(II) complexes of the macrocyclic ligand TAAB ($[FeTAAB(L)_2](PF_6)_2$, L = methylimidazole, pyridine, acetonitrile, and benzyl isocyanide, and $[FeTAAB(L)(X)](PF_6)_2$, X = CO). The complexes undergo axial ligand substitution reactions via a dissociative mechanism in acetonitrile and acetone solution. Stability constants and rate constants for CO and BzlNC binding are compared with analogous data for phthalocyanine, porphyrin, and dimethylglyoxime systems. Of the heme models studied the TAAB system is the poorest at binding axial π acceptors.

Introduction

Previous work has shown that axial ligand substitution reactions of tetragonal low-spin Fe(II) complexes of macrocyclic ligands for phthalocyanine,[1-3] porphyrin,[4,5] and glyoxime[6,7] systems proceed by a dissociative mechanism. The existence of comparable data for methylimidazole, carbon monoxide, and benzyl isocyanide binding to these systems allows for a detailed comparison of the effects of a macrocyclic ligand on the stability and lability of axial ligands. In these systems, differences of the order of 10^5 in stability constant

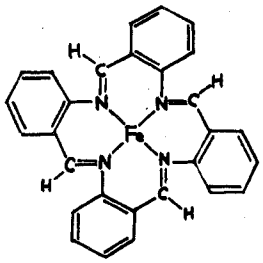

Figure 1. Structure of $Fe(TAAB)^{2+}$.

or rate constants as a function of the in-plane ligand are observed. Herein we report analogous data for ferrous TAAB, one of several synthetic macrocycles originally prepared by Busch and co-workers.[8] While TAAB has been compared with porphyrins,[9] no previous report of axial ligation to this system has appeared except for a report of the synthesis of a bis(acetonitrile) complex.[10]

Like most of the synthetic macrocycles, the FeTAAB complex has a +2 charge in contrast to the previously studied systems which are all neutral. Another interesting feature of TAAB is its extensive ring puckering in the solid state and its considerable hole size flexibility evident from structures of two nickel complexes, one high spin with a Ni–N distance of 2.10 Å and the other low spin with a Ni–N distance of 1.90 Å.[11]

Experimental Section

Materials. 1-Methylimidazole (Aldrich) and pyridine (Fisher) were distilled from KOH prior to use. Acetone and butanone (BDH Analar) were dried over molecular sieves (3 Å). Carbon monoxide (Matheson C. P.), acetonitrile (Matheson Spectroquality), and ammonium hexafluorophosphate (Ozark-Mahoning) were used as received. Benzyl isocyanide was prepared via the formamide.[12]

Physical Measurements. Visible spectra were recorded on a Cary 14 spectrophotometer. Infrared spectra were obtained as Nujol mulls with a Beckman IR-12. NMR spectra were obtained on a Varian HA-100 or Em-360 spectrometer using deuterioacetone or deuterioacetonitrile as solvent. Elemental analyses were performed by Chemalytics, Tempe, Ariz.

Syntheses of Fe^{II}–TAAB Complexes. $Fe(TAAB)FeCl_4$. Anhydrous iron(II) chloride (0.83 g, 0.0066 mol) was dissolved in 9 mL of absolute alcohol with concentrated HCl (0.03 mL) under nitrogen. An absolute alcohol solution (4 mL) of freshly prepared *o*-aminobenzaldehyde (1.6 g, 0.0132 mol) was slowly added to the iron(II) chloride solution. The solution immediately turned orange-red and then dark-green on heating. After refluxing for 6 h, the solution was filtered to give a dark green solid. This was washed with 30 mL of absolute alcohol and dried in vacuo, yield 1.13 g. IR (cm^{-1}), three doublets, 1618 (s), 1591 (m), 1566 (m). This product, which has been briefly described previously,[9,10] was not pure. However, it served as a convenient starting material for the following syntheses.

$Fe(TAAB)(CH_3Im)_2(PF_6)_2$. $Fe(TAAB)FeCl_4$ (2.0 g, 0.0030 mol) and NH_4PF_6 (1.0 g, 0.0061 mol) were dissolved in a mixed solution of 8 mL of acetonitrile and 2 mL of 1-methylimidazole. The filtrate of the deep blue solution was eluted through an alumina column with a solvent mixture of $(C_2H_5)_2O$:CH_3CN:CH_3Im = 70:25:5 (v/v) (CH_3Im was added in order to prevent the replacement of coordinated CH_3Im by CH_3CN). The elution was followed by visible spectroscopy. Initial blue fractions, which give a λ_{max} at 590 nm, were collected. The solution was then concentrated to ~10 mL and 100 mL of diethyl ether added. Cooling the solution gave dark blue crystals, yield 0.65 g (24%). Anal. Calcd for $C_{36}H_{32}N_8P_2F_{12}Fe$: C, 46.87; H, 3.50; N, 12.15. Found: C, 45.21; H, 3.33; N, 10.20. NMR (CD_3CN, δ Me_4Si) 3.23 (CH_3, 6 H), 6.38, 6.58, 7.30 (CH_3Im, 2 H each), 7.5 (m) (TAAB, 16 H), 9.26 (TAAB, 4 H). Molar conductance at 9.63×10^{-4} M in acetonitrile, Λ = 272 Ω^{-1} M^{-1}.

$Fe(TAAB)(py)_2(PF_6)_2$ was prepared with a similar procedure as above; 5% pyridine in acetone (v/v) was used as the eluent. Anal. Calcd for $C_{38}H_{30}N_6P_2F_{12}Fe$: C, 49.80; H, 3.30; N, 9.17. Found: C, 49.97; H, 3.49; N, 10.22. NMR (CD_3CN, δ Me_4Si) 6.85 (py, 4 H), 7.70 (py, 2 H), 7.47 (m) (TAAB, 16 H), 8.38 (py, 4 H), 9.30 (TAAB, 4 H).

$Fe(TAAB)(CH_3CN)_2(PF_6)_2$ was prepared with a similar procedure as above except pure acetonitrile was used as the eluent. Anal. Calcd for $C_{32}H_{26}N_6P_2F_{12}Fe$: C, 45.74; H, 3.12; N, 10.00. Found: C, 45.58; H, 3.39; N, 9.66. NMR (CD_3CN, δ Me_4Si) 1.95 (CH_3CN, overlaps solvent resonance), 7.72 (m) (TAAB, 16 H), 9.20 (TAAB, 4 H).

$Fe(TAAB)(CH_3CN)(BzlNC)(PF_6)_2$. $Fe(TAAB)(CH_3CN)_2(PF_6)_2$ (0.33 g, 0.000 39 mol) was dissolved in acetonitrile (25 mL), and benzyl isocyanide (0.30 g, 0.0025 mol) was added to this solution. The solution gave a spectrum with λ_{max} at 520 and 615 nm immediately. Upon addition of diethyl ether and cooling, the solution gave dark red crystals. The crystals were washed with diethyl ether and dried in vacuo, yield 0.3 g (90%). Anal. Calcd for $C_{38}H_{30}N_6P_2F_{12}Fe$: C, 49.80; H, 3.30; N, 9.17. Found: C, 50.26; H, 3.84; N, 8.72. NMR (CD_3CN, δ Me_4Si) 1.95 (CH_3CN, overlaps solvent resonance), 4.37 (BzlNC, 2 H), 6.7–7.3 (m) (BzlNC, 5 H), 7.65–7.7 (m) (TAAB, 16 H), 8.75 (TAAB, 2 H), 8.95 (TAAB, 2 H).

$Fe(TAAB)(CH_3Im)(BzlNC)(PF_6)_2$, was prepared with a similar procedure as above. Anal. Calcd for $C_{40}H_{33}N_7P_2F_{12}Fe$: C, 50.17; H, 3.47; N, 10.24. Found: C, 50.34; H, 3.71; N, 10.98. NMR (CD_3CN, δ Me_4Si) 3.33 (CH_3, 3 H), 4.43 (BzlNC, 2 H), 6.58 (CH_3Im, 1 H), 6.8–7.7 (m) (TAAB + CH_3Im + BzlNC, 16 H + 2 H + 5 H), 8.82 (TAAB, 2 H), 9.02 (TAAB, 2 H).

$Fe(TAAB)(py)(BzlNC)(PF_6)_2$ was prepared with a similar procedure as above. Anal. Calcd for $C_{41}H_{32}N_6P_2F_{12}Fe$: C, 51.59; H, 3.38; N, 8.80. Found: C, 51.37; H, 3.35; N, 8.93. NMR (CD_3CN, δ Me_4Si) 4.47 (BzlNC, 2 H), 6.90 (py, 2 H), 7.4–7.8 (TAAB + py + BzlNC, 16 H + 1 H + 5 H), 8.5 (py, 2 H), 8.95 (TAAB, 2 H), 9.15 (TAAB, 2 H).

$Fe(TAAB)(BzlNC)_2(PF_6)_2$ was prepared in the same way as $Fe(TAAB)(CH_3CN)(BzlNC)(PF_6)_2$ except acetone was used instead of acetonitrile. Recrystallization was carried out in acetone and diethyl ether. Anal. Calcd for $C_{44}H_{34}N_6P_2F_{12}Fe$: C, 53.24; H, 3.45; N, 8.47. Found: C, 52.64; H, 3.58; N, 8.21. NMR (CD_3CN, δ Me_4Si) 4.40 (BzlNC, 4 H), 6.83–7.46 (BzlNC, 10 H), 7.7 (m) (16 H), 8.77 (TAAB, 4 H).

Kinetic and Equilibrium measurements were made by visible spectroscopy using procedures analogous to those described previously.[3]

Results and Discussion

$Fe(TAAB)FeCl_4$ is employed as the starting material for making all the six-coordinate TAAB complexes. The product gives three intense bands around 1600 cm^{-1}—the typical IR absorption pattern of metal TAAB complexes.[8] The Fe(TAAB) complexes prepared in this work, except the low-spin bis(acetonitrile) complex,[10] are new compounds. They are stable in the solid state and for at least 24 h in acetonitrile solution. The proposed structures for the synthesized complexes are fully supported by elemental analysis and NMR. The incorporation of PF_6^- in the complexes is supported by the strong IR band at 845 cm^{-1}. The conductance was measured in the case of $Fe(TAAB)(CH_3Im)_2(PF_6)_2$ in acetonitrile and found to be 272 Ω M^{-1}. The value is expected for a 1:2 electrolyte in this solvent[13] and indicates the complex is completely dissociated under these conditions.

Six-coordinate Fe^{II}–TAAB complexes are soluble in acetonitrile, acetone, and butanone in which all the kinetic and equilibrium studies were carried out. However, many of the ligands in the complexes are subject to the replacement by either the water in the ketonic solvents or acetonitrile. We have taken precautions where necessary to prevent such coordination which would interfere with the kinetics.

All of the six-coordinate Fe^{II}–TAAB complexes, except the carbonyl complexes, display an absorption pattern with an intense band (ϵ 4×10^3 M^{-1} cm^{-1}, containing a shoulder) between 500 and 600 nm (band A) and a less intense band (ϵ 2×10^3 M^{-1} cm^{-1}) at longer wavelength (band B) as shown in Table I. Band A has been previously observed in the spectra of metal TAAB complexes and their derivatives[8,9] and is assigned to a charge-transfer transition. Whether band B is a d–d transition band or a metal–ligand charge-transfer band is uncertain.

There exists a general trend in Fe(TAAB) as well as Fe(DMGH)$_2$[7] and Fe(TIM) systems[14,15] that as the donor

Table I. Visible Spectral Data for Fe^{II}-TAAB Complexes

	λ_{max}, nm ($10^{-3}\epsilon$, M^{-1} cm^{-1})			Solvent
	Band A		Band B	
$Fe(TAAB)(CH_3Im)^{2+}$	591 (5.2)	550 sh	850 (2.4)	*a*
$Fe(TAAB)(py)_2^{2+}$	567 (4.6)	535 sh	750 (2.1)	*b*
$Fe(TAAB)(CH_3CN)_2^{2+}$	522 (4.7)	487 sh	665 (2.3)	*c*
$Fe(TAAB)(CH_3Im)(BzlNC)^{2+}$	548 (4.2)	512 sh	662 (2.2)	*c*
$Fe(TAAB)(py)(BzlNC)^{2+}$	536 (4.1)	505 sh	635 (2.0)	*c*
$Fe(TAAB)(CH_3CN)(BzlNC)^{2+}$	521 (4.4)	487 sh	615 (2.2)	*c*
$Fe(TAAB)(BzlNC)_2^{2+}$	523 (4.9)	475 sh	590 (2.3)	*c*
		450 sh		
$Fe(TAAB)(CH_3Im)(CO)^{2+}$	480 (~4)			*d*
$Fe(TAAB)(py)(CO)^{2+}$	475 (~4)			*d*
$Fe(TAAB)(CH_3CN)(CO)^{2+}$	470 (~4)			*e*
$Fe(TAAB)(H_2O)(BzlNC)^{2+}$	525 (~4)	490 sh	650 (~2)	*f*

[a] Acetonitrile solution with 1% 1-methylimidazole. [b] Acetonitrile solution with 1% pyridine. [c] Acetonitrile solution. [d] Acetone solution under 760 Torr of CO. [e] Acetone solution with 3% acetonitrile under 760 Torr of CO. [f] Acetone solution.

Table II. Chemical Shift of the Aldehydic Protons of Fe^{II}-TAAB Complexes in Deuterioacetonitrile

	δ(-C(H)=N)
$Fe(TAAB)(CH_3Im)_2^{2+}$	9.27
$Fe(TAAB)(py)_2^{2+}$	9.30
$Fe(TAAB)(CH_3CN)_2^{2+}$	9.20
$Fe(TAAB)(BzlNC)_2^{2+}$	8.77
$Fe(TAAB)(CH_3Im)(BzlNC)^{2+}$	8.82, 9.02
$Fe(TAAB)(py)(BzlNC)^{2+}$	8.95, 9.15
$Fe(TAAB)(CH_3CN)(BzlNC)^{2+}$	8.75, 8.95

strength of axial ligands decreases, or π-acceptor strength increases, the major spectral band assigned to change transfer from metal to in-plane ligand shifts toward shorter wavelength. This is understandable since the ease of charge transfer from iron to TAAB is proportional to the electron density at iron, which is a function of σ-donor as well as π-acceptor properties of axial ligands.

NMR. This is the first reported NMR study of TAAB complexes. The spectra typically show the resonances of the phenyl protons and the aldehydic protons of TAAB at δ 7.4–7.8 and 8.7–9.3, respectively. Coordinated benzyl isocyanide displays its benzylic proton resonance and its phenyl proton resonances slightly upfield of the free ligand. Coordinated amines give a similar resonance pattern as the free amines but with substantial upfield shifts.

The most interesting feature in the NMR is that the four aldehydic protons of TAAB are differentiated into two sets, when the two axial ligands are different (Table II). This suggests the protons are not in the same plane and thus subject to different shielding effects. This finding is consistent with the S_4 symmetry of TAAB in the solid state.[11] The TAAB ligand is puckered in solution, with two protons directed above and two below the approximate plane of the nitrogens. The interconversion of the two types of aldehydic protons is slow on the NMR time scale indicating that a substantial energy barrier exists to a flattening of the TAAB ligand on iron.

The upfield shift of coordinated ligands and the nonequivalence of the aldehydic resonances of TAAB in mixed complexes make NMR a particularly diagnostic technique in this system. We have followed the substitution reactions

$$FeTAAB(CH_3Im)_2^{2+} + BzlNC \rightarrow Fe(TAAB)(CH_3Im)(BzlNC)^{2+} + CH_3Im$$

$$FeTAAB(py)_2^{2+} + BzlNC \rightarrow FeTAAB(py)(BzlNC)^{2+} + py$$

$$FeTAAB(CH_3CN)_2^{2+} + BzlNC \rightarrow FeTAAB(CH_3CN)(BzlNC)^{2+} + CH_3CN$$

$$FeTAAB(CH_3CN)(BzlNC)^{2+} + BzlNC \rightarrow FeTAAB(BzlNC)_2^{2+} + CH_3CN$$

by addition of BzNC to NMR tubes containing the complexes in deuterioacetonitrile. In all cases these reactions proceed cleanly with resonances of free ligand and coordinated ligand clearly discernible in most cases. The changes in the aldehydic region of the TAAB ligand are also diagnostic. For example, in the case of the acetonitrile complex one observes a fast reaction complete on mixing giving $FeTAAB(CH_3CN)(BzlNC)^{2+}$ (the singlet at δ 9.20 disappears and two resonances appear at δ 8.75 and 8.95). A slower reaction then results in the loss of these two resonances and only a singlet appears in the final spectrum at δ 8.76. These observations are in all cases fully consistent with rates and assignments made on the basis of visible spectroscopic measurements and with the NMR spectra of isolated samples of the pure complexes.

Kinetics. The kinetics of axial ligation have been treated on the assumption that the reactions proceed via the same dissociative mechanism previously shown for other heme models.[1-7]

$$Fe(TAAB)L_2^{2+} \underset{k^{-1}}{\overset{k_1}{\rightleftharpoons}} Fe(TAAB)L^{2+} \underset{k^{-2}}{\overset{k_2}{\rightleftharpoons}} Fe(TAAB)(L)(X)^{2+}$$

For such a mechanism the observed pseudo-first-order rate constant neglecting the reverse reaction is given by

$$k_{obsd} = \frac{k_1 k_2 [X]}{k_{-1}[L]} \Big/ \left(1 + \frac{k_2[X]}{k_{-1}[L]}\right)$$

At high concentration of X the observed rate becomes independent of [X] and $k_{obsd} = k_1$, the dissociative rate constant for L. At low [X]/[L], the rate becomes first order in [X]. For intermediate values of the ratio [X]/[L] the pseudo-first-order rate constant may be analyzed to give both k_1 and the relative on-rates, $k_2/(k_{-1})$. The equilibrium constant for the overall reaction is related to the rate constants by $K = k_1k_2/k_{-1}k_{-2}$. For the reactions to be described, in some cases a complete study of the dependence of k_{obsd} on [L]/[X] has been carried out and compared with the static determination of the equilibrium constant. In all other cases, k_{obsd} has been shown to be invariant to a tenfold change in the concentration of the added ligand under the conditions of the kinetics. This ensures that the observed pseudo-first-order rate constant is identified with the rate constant for dissociation of the leaving group from the complex. The reactions were carried out at FeTAAB concentrations of typically 2×10^{-4} M in order to give solutions with absorbances in 1-cm cells of about 1.0 at the absorbance maxima. All reactions proceed cleanly to completion giving isosbestic points in the visible spectra and linear log plots from which k_{obsd} is obtained.

$FeTAAB(L)_2^{2+} + BzlNC \rightarrow FeTAAB(L)(BzlNC)^{2+} + L$. If a concentrated acetonitrile solution of $Fe(TAAB)(CH_3Im)_2^{2+}$ is diluted with acetonitrile slow spectral changes are observed assigned to the incomplete reaction $Fe(TAAB)(CH_3Im)_2^{2+} + CH_3CN = Fe(TAAB)(CH_3Im)(CH_3CN)^{2+} + CH_3Im$. This incomplete reaction is inconvenient for kinetics. If the concentrated solution is diluted with a solution of 0.1 M BzlNC in acetonitrile a clean and complete reaction is observed giving only $Fe(TAAB)(CH_3Im)(BzlNC)^{2+}$. No evidence for acetonitrile coordination is observed during the course of the reaction since the concentration of BzlNC is sufficiently high to make the reaction of the intervening acetonitrile complex rapid under these conditions. Clean isosbestic points indicate that only the initial $FeTAAB(CH_3Im)_2^{2+}$ complex and the final $FeTAAB(CH_3Im)(BzlNC)^{2+}$ are present in significant amounts during the reaction. While the reaction almost certainly proceeds via the $Fe(TAAB)(CH_3Im)(CH_3CN)^{2+}$ complex, the rate-determining step at these conditions is the dissociation of CH_3Im from the starting complex. The rate of the reaction is in-

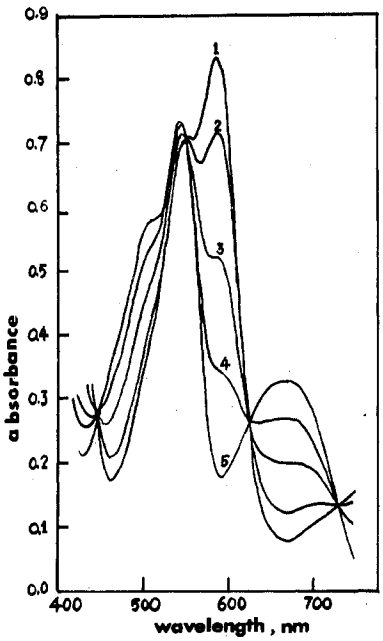

Figure 2. Spectral changes with time for the reaction Fe(TAAB)-$(CH_3Im)_2^{2+}$ + BzlNC = Fe(TAAB)$(CH_3Im)(BzlNC)^{2+}$ + CH_3Im in acetonitrile at 10 °C. Spectra 1–5 recorded at times 0, 5, 17, 36, and 240 min.

dependent of the concentration of BzlNC at concentrations greater than 0.01 M. Typical spectral changes with time on addition of benzyl isocyanide to a Fe(TAAB)$(CH_3Im)_2^{2+}$ solution at 10 °C are given in Figure 2. As the absorbance of Fe(TAAB)$(CH_3Im)_2^{2+}$ at 590 nm decreases, the 670-nm peak due to Fe(TAAB)$(CH_3Im)(BzlNC)^{2+}$ increases. The analyses at 590 and 670 nm give consistent rate constants.

The substitution reaction of Fe(TAAB)$(py)_2^{2+}$ with benzyl isocyanide also carried out in acetonitrile proceeds similarly with a decrease in absorbance at 750 nm and an increase in absorbance at 650 nm, corresponding to the formation of Fe(TAAB)(py)$(BzlNC)^{2+}$. The analyses at these two wavelengths are also in good agreement.

For both 1-methylimidazole and pyridine complexes, plots of log $(A_0 - A_\infty)/(A - A_\infty)$ vs. time are linear for 3 half-lives. Plots of ln k/T vs. $1/T$ were obtained. The derived rate constants and activation parameters are given in Table III.

A complete study of the reaction of the bis(methylimidazole) complex with BzlNC has been carried out in butanone at 25 °C. The reaction has been investigated at constant CH_3Im (0.01 M) and varying BzlNC (0.003–0.1 M). Linear plots of k_{obsd}^{-1} vs. $[CH_3Im]/[BzlNC]$ consistent with the assumed dissociative mechanism are analyzed for the CH_3Im dissociation rate constant, $k_{-CH_3Im} = 3.3 \times 10^{-3}$ s^{-1}, and the relative on-rates, $k_{+BzNC}/k_{+CH_3Im} = 0.64$.[16] The value 0.64 indicates a small preference of the five-coordinate intermediate Fe-(TAAB)CH_3Im^{2+} for CH_3Im over BzlNC. The value of k_{-CH_3Im} in butanone is approximately a factor of 2 slower than that obtained in acetonitrile.

The equilibrium constant for

$$FeTAAB(CH_3Im)_2^{2+} + BzlNC = FeTAAB(CH_3Im)(BzlNC)^{2+} + CH_3Im$$

was obtained from visible spectra of solutions of FeTAAB-$(CH_3Im)_2^{2+}$ (2×10^{-4} M) in butanone at 25 °C containing 0.80 M CH_3Im and varying amounts of BzlNC (0.001–0.1 M). The solutions were allowed to equilibrate for 48 h in the dark. Spectral data showing good isosbestic points were analyzed at 590 nm. A plot of log $(A_0 - A)/(A - A_\infty)$ vs. log $[CH_3Im]/[BzlNC]$ is linear with slope of 1.0 consistent with the proposed equilibrium. The equilibrium constant $K = 58$

Table III. Kinetic Data for the Reactions of Fe^{II}–TAAB Complexes

Complexes[a]	Entering group	Solvent	$10^4 k$, s^{-1} 10 °C	15 °C	20 °C	25 °C	30 °C	40 °C	50 °C	60 °C	$\Delta H^{\ddagger}$, kcal/mol	$\Delta S^{\ddagger}$, eu
Fe(TAAB)$(CH_3Im)CH_3Im^{2+}$	BzlNC	Acetonitrile	6.33 (6)			69 (1)		605 (15)			26.2 (1)	19.5 (4)
Fe(TAAB)$(CH_3Im)BzlNC^{2+}$	BzlNC	Butanone				33 (1)	64 (2)					
Fe(TAAB)$(CH_3Im)CH_3Im^{2+}$	CH_3Im	Butanone					0.80 (6)	4.8 (1.2)	17 (4)	56 (5)	28 (1)	15 (4)
Fe(TAAB)$(BzlNC)CH_3Im^{2+}$	BzlNC	Butanone								0.33 (1)		
Fe(TAAB)$(BzlNC)BzlNC^{2+}$	CH_3Im	1-Methylimidazole								128 (10)		
Fe(TAAB)$(py)py^{2+}$	BzlNC	Acetonitrile	27.9 (4)	68 (3)	152 (2)	346 (2)					27.1 (1)	26.5 (4)
Fe(TAAB)$(BzlNC)CH_3CN^{2+}$	BzlNC	Acetone				133 (10)						

[a] Leaving ligand without parentheses.

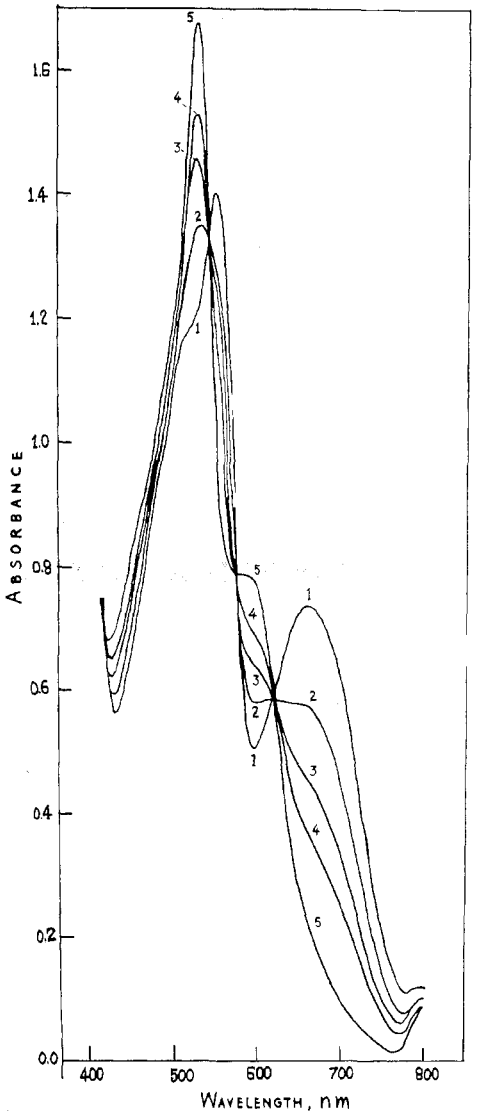

Figure 3. Spectral changes with time for the reaction Fe(TAAB)$(CH_3Im)(BzlNC)^{2+}$ + BzlNC = $Fe(TAAB)(BzlNC)_2^{2+}$ + CH_3Im in butanone at 60 °C. For decreasing absorbance at 662 nm times are 0, 2.8, 6.3, 10.3, and 49 h.

± 6 is in excellent agreement with that calculated from the kinetic data in this solvent at 25 °C. $K_{calcd} = k_1k_2/k_{-1}k_{-2}$ = 54.

$Fe(TAAB)(CH_3Im)(BzlNC)^{2+}$ + BzlNC. Typical spectral changes with time on addition of benzyl isocyanide to a $Fe(TAAB)(CH_3Im)(BzlNC)^{2+}$ solution in butanone are shown in Figure 3. They are consistent with the formation of $Fe(TAAB)(BzlNC)_2^{2+}$ and indicate no decomposition of the complexes in the period of 2 days at 60 °C under the experimental conditions. Analyses at 675 and 525 nm give a rate constant of 3.3×10^{-5} s^{-1} at 60 °C.

$Fe(TAAB)(CH_3Im)(BzlNC)^{2+}$ + CH_3Im. The reaction of $Fe(TAAB)(CH_3Im)(BzlNC)^{2+}$ with 1-methylimidazole was carried out in butanone. Typical spectral changes for this reaction are the reverse of those in Figure 2. Linear log plots are obtained. Unlike the other reactions, there is a slight dependence of the reaction rate on the concentration of the entering ligand. By varying $[CH_3Im]$ from 0.1 to 1 M, the rate of the reaction, at various temperatures, increases by 15–50%. The small change of rate constants over a tenfold variation of $[CH_3Im]$ is inconsistent with a S_N2 mechanism. It is suggested that the reaction proceeds via a dissociative mechanism, and the small dependence of rate on $[CH_3Im]$ is due to a solvent effect. The derived activation parameters together with the rate constants are given in Table III. As the rate is slightly dependent on $[CH_3Im]$, the rate constants given are the average of those obtained at three concentrations, i.e., 0.1, 0.3, and 1.0 M.

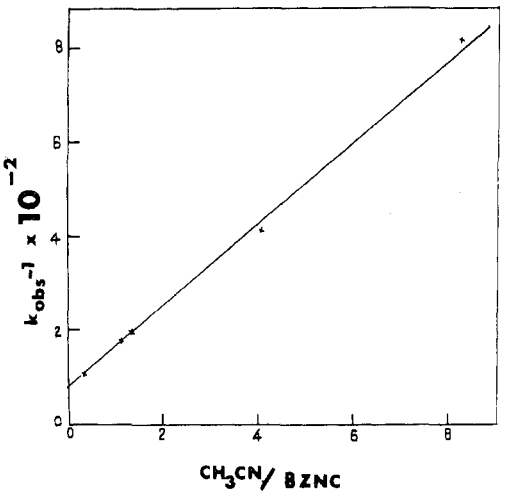

Figure 4. Plot of k_{obsd}^{-1} vs. CH_3CN/BzlNC for the reaction Fe$(TAAB)(CH_3CN)(BzlNC)^{2+}$ + BzlNC = $Fe(TAAB)(BzlNC)_2^{2+}$ + CH_3CN in acetone at 25 °C.

$Fe(TAAB)(BzlNC)_2^{2+}$ + CH_3Im. The reaction was studied in neat 1-methylimidazole. The reaction is characterized by a decrease in absorbance at 525 nm due to the disappearance of $Fe(TAAB)(BzlNC)_2^{2+}$ and a corresponding increase in absorbance at 590 nm due to $Fe(TAAB)(CH_3Im)_2^{2+}$ and a loss of isosbestic points. This is attributed to the comparable rate of the two substitution reactions

$$Fe(TAAB)(BzlNC)_2^{2+} + CH_3Im \rightleftharpoons Fe(TAAB)(CH_3Im)(BzlNC)^{2+} + BzlNC$$

$$Fe(TAAB)(CH_3Im)(BzlNC)^{2+} + CH_3Im \rightleftharpoons Fe(TAAB)(CH_3Im)_2^{2+} + BzlNC$$

Problems due to the intervention of the second substitution can be eliminated by analysis at a wavelength (730 nm) where $Fe(TAAB)(CH_3Im)(BzlNC)^{2+}$ and $Fe(TAAB)(CH_3Im)_2^{2+}$ have identical extinction coefficients and $Fe(TAAB)(CH_3Im)(BzlNC)^{2+}$ and $Fe(TAAB)(BzlNC)_2^{2+}$ have significantly different extinction coefficients. The analysis at 730 nm gives linear log plots for 3 half-lives. The rate constant thus obtained is 1.28×10^{-2} s^{-1} at 60 °C.

$Fe(TAAB)(CH_3CN)(BzlNC)^{2+}$ + BzlNC. The reaction is characterized by a shift of the band at 615 nm to 590 nm, corresponding to the formation of $Fe(TAAB)(BzlNC)_2^{2+}$. Kinetics were carried out in acetone solution in the presence of varying concentrations of acetonitrile (0.2–1.2 M) and benzyl isocyanide (0.02–0.5 M). A linear plot of k_{obsd}^{-1} vs. $[CH_3CN]/[BzlNC]$ (Figure 4) gives a dissociative rate constant k_{-CH_3CN} of 1.33×10^{-2} s^{-1} and a relative on-rate k_{+BzlNC}/k_{+CH_3CN} of 0.88 at 25 °C. The value of 0.88 reflects a slight preference of addition of CH_3CN over BzNC to the intermediate $FeTAAB(BzlNC)^{2+}$.

Carbonyl Complexes. The binding of CO to FeTAAB complexes according to the equilibrium

$$FeTAAB(L)_2^{2+} + CO = FeTAAB(L)(CO)^{2+} + L$$

is very poor. Only in the case L = CH_3CN have we isolated a carbonyl complex. This complex gives a strong, sharp CO stretch in the IR region at 2038 cm^{-1} and is converted to the $FeTAAB(L)_2^{2+}$ complexes in the presence of excess L, L = CH_3CN, CH_3Im, or py. A low nitrogen analysis, however, suggests that the isolated complex is not pure and may contain

coordinated H_2O instead of CH_3CN.

Despite the weak binding of CO to this system, we have been able to obtain good kinetic data and qualitative equilibrium data by generating the carbonyl complexes in situ. Experiments were carried out in acetone solution since the solubility of CO is known in this solvent (1.05×10^{-2} M (760 Torr)).[17] In all cases the identification of the carbonyl species is associated with the appearance of a visible band at 480 nm and a corresponding decrease in the visible band of the Fe-TAAB$(L)_2^{2+}$ complex. These changes are reversible by either pumping off the CO or adding excess L.

Spectra of solutions of Fe$TAAB(CH_3CN)_2^{2+}$ in CO-saturated acetone containing varying concentrations of acetonitrile (0.1–2.0 M) were analyzed at 665 nm by substituting absorbances into the expression $K = (A_0 - A)(CH_3CN)/(A - A_\infty)(CO)$. The values of A_∞, the absorbance of pure Fe-TAAB$(CH_3CN)(CO)^{2+}$, and K are calculated. The equilibrium constant $K = 86$, while approximate, provides a reasonably quantitative measure of the binding of CO to Fe$TAAB(CH_3CN)_2^{2+}$ for comparison with other data. Changes in spectra on addition of excess CH_3CN are complete on mixing, indicating k_{-CO} is greater than 0.1 s^{-1}.

The binding of CO to Fe$TAAB(py)_2^{2+}$ and Fe$TAAB(CH_3Im)_2^{2+}$ is much poorer than the acetonitrile case. Almost no spectral change is observed on addition of 760 Torr of CO to a 1-cm cell of Fe$TAAB(CH_3Im)_2^{2+}$ (2×10^{-4} M) in acetone, and only a slight change is observed for Fe$TAAB(py)_2^{2+}$. If the reaction is carried out in a 5-cm cell at 6.5×10^{-5} M, these changes are greater, consistent with the shift of the equilibrium expected on dilution. The equilibrium constants for CO binding to the Fe$TAAB(CH_3Im)_2^{2+}$ and Fe$TAAB(py)_2^{2+}$ complexes are estimated as 3×10^{-4} and 9×10^{-3}, respectively, based on these spectral changes in the presence of CO. Typical data for the Fe$TAAB(py)_2^{2+}$ complex are given in Figure 5. After addition of pyridine (0.02–0.2 mL), the reaction is followed by the decrease in absorbance at 485 nm or the increase in absorbance at 565 nm.

The final spectrum is consistent with the Fe$(TAAB)(py)_2^{2+}$ complex. Analyses at both wavelengths give a rate constant of 2.5×10^{-2} s^{-1} at 20 °C independent of the pyridine concentration.

The reaction solution of Fe$(TAAB)(CH_3Im)(CO)^{2+}$ prepared by addition of CO to Fe$(TAAB)(CH_3Im)_2^{2+}$ gives very small absorbance changes. A solution containing greater than 80% Fe$TAAB(CH_3Im)(CO)^{2+}$ can be prepared as follows. Upon addition of Fe$(TAAB)(CH_3CN)_2^{2+}$ (0.0006 g, 7.3×10^{-7} mol) to 3 mL of Fe$(TAAB)(CH_3Im)_2^{2+}$ (0.0006 g, 6.5×10^{-7} mol) in acetone under 760 Torr of CO, the absorbance at 588 nm due to Fe$(TAAB)(CH_3Im)_2^{2+}$ slowly decreases with the emerging of a peak at ~480 nm, characteristic of the absorption of carbonyl complexes in this system. The possibilities of the presence of a significant amount of Fe-$(TAAB)(H_2O)(CO)^{2+}$ and/or Fe$(TAAB)(CH_3CN)(CO)^{2+}$ in solution are eliminated by the subsequent kinetics. (Both of these carbonyl dissociations are too fast to be followed at 10 °C). The CO dissociation from Fe$(TAAB)(CH_3Im)(CO)^{2+}$ was carried out by adding 1-methylimidazole (0.01–0.1 g) to the solution and following the increase in absorbance at 590 nm. The final spectrum is identical with that of Fe-$(TAAB)(CH_3Im)_2^{2+}$. A rate constant of 6.5×10^{-3} s^{-1} at 20 °C is obtained. That there is no immediate increase in absorbance at 590 nm at the beginning of the reaction implies little or no aquo or acetonitrile complexes in the solution for they would be converted to the Fe$(TAAB)(CH_3Im)_2^{2+}$ complex rapidly ($t_{1/2} < 10$ s) under these conditions.

Comparison with Other Heme Models. Kinetic and equilibrium data for various heme models are given in Table IV. Taking into account small differences due to different solvents a reasonable measure of the large range of differences possible with changes in the in-plane ligand may be obtained.

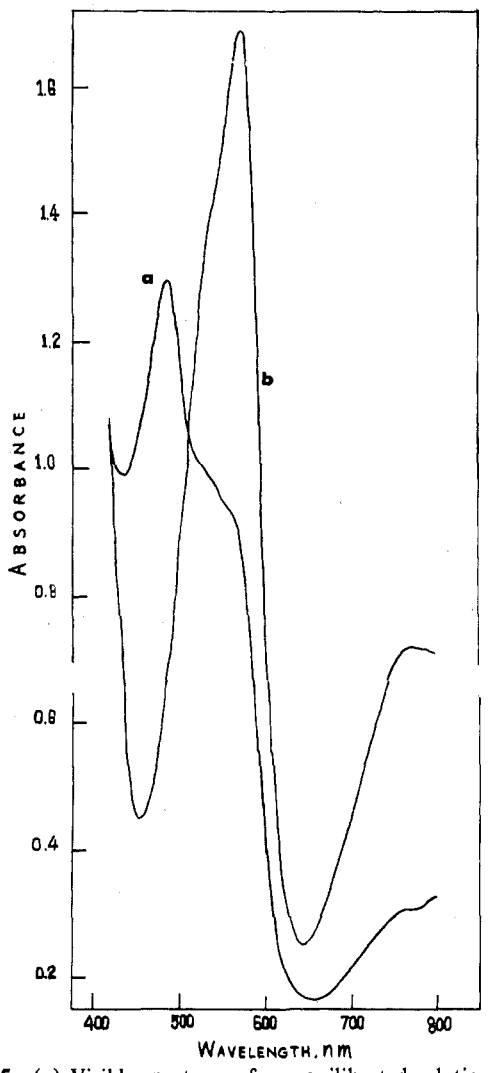

Figure 5. (a) Visible spectrum of an equilibrated solution of Fe-$(TAAB)(py)_2^{2+}$ (6.5×10^{-5} M) in CO-saturated acetone in a 5-cm pathlength cell at 20 °C. (b) Spectrum of solution after completion of the reaction with pyridine (0.1 M).

The equilibrium constant for CO binding to myoglobin is the largest and should not be compared with the models since no ligand is displaced in the protein reaction. The iron porphyrins bind CO the best with equilibrium constants of the order of 10^4 depending on the axial ligand and solvent. The only other systems which even come close to the iron porphyrins in binding CO are the glyoxime systems with a $K_{CO} = 43$. The phthalocyanine system is much poorer and the TAAB system is clearly the worst. For BzlNC binding the porphyrins are better than Pc, better than TAAB. While a quantitative measure of the equilibrium for the DMGH system was not obtained, qualitative observations indicate it is comparable to the porphyrins. These results are in agreement with CO and NC stretching frequencies (Table V).

A markedly different picture is obtained if the lability of ligands is considered. The lability of the amines, methylimidazole, pyridine, etc. are sufficiently similar in many of the systems that some differences may be a result of the different solvents used. However, the porphyrins appear to be the most labile. For CO dissociation, the porphyrins and phthalocyanines are comparable to the protein. The TAAB system which is the worst at binding CO thermodynamically is somewhat more inert with respect to CO dissociation, and the

Table IV. Comparison of the Kinetic and Equilibrium Data of the Reaction

$$Fe(N_4)L_2 + X(CO, BzlNC) \underset{k_{+L}}{\overset{k_{-L}}{\rightleftharpoons}} Fe(N_4)L \underset{k_{-X}}{\overset{k_{+X}}{\rightleftharpoons}} Fe(N_4)LX$$

for Various Heme Models[i]

$Fe(N_4)$	L	k_{-L} (°C)	k_{-CO} (°C)	k_{-BzlNC} (°C)	K_{CO}	K_{BzlNC}
$Fe(DMGH)_2$[a]	C_4H_3Im	6.9×10^{-4} (10)	2.5×10^{-6} [j]	4.6×10^{-4} (65)		
	py	7.0×10^{-3} (10)	1.0×10^{-5} [j]	3.1×10^{-4} (65)		
$Fe(DPGH)_2$[b]	py	4×10^{-3}	2.5×10^{-5}		43	
Fe(TAAB)	CH_3Im	3.3×10^{-3}	6.5×10^{-3} (20)	3.9×10^{-5} [j]	3×10^{-4}	58
	py	3.4×10^{-2}	2.5×10^{-2} (20)		9×10^{-3}	
Fe(Pc)[c]	CH_3Im	1.3×10^{-3}		3×10^{-5} [j]		4.0×10^2
	Im	2.5×10^{-3}	0.02		0.03	
	py	0.12	0.09	6×10^{-5} [j]	0.37	3.2×10^3
	pip	0.50	0.13	1.6×10^{-4}	0.85	3.2×10^3
Deuteroheme[d]	Im				7×10^3	
Fe(PPIX)[e]	pip	20	0.06		2.3×10^5	
Fe(TPP)	pip[e]	11	0.52	>0.01[h]	1.5×10^4	~4×10^4 [h]
	pip[f]	2.8×10^{-4} (−79)	$<4 \times 10^{-6}$ (−79)		>750	
	CH_3Im[f]	6.1×10^{-6} (−79)	$<2 \times 10^{-7}$ (−79)		>160	
	py[f]	6.6×10^{-5} (−79)	$<2 \times 10^{-7}$ (−79)		>2600	
Myoglobin[g]			0.017 (20)	0.23 (19)	2.9×10^7	2×10^5

[a] Reference 7, k_{-L} chloroform, k_{-CO} k_{-BzlNC} methylimidazole or pyridine. [b] Reference 6, chlorobenzene. [c] References 1 and 3, toluene (23 °C). [d] M. Rougee and D. Brault, *Biochemistry*, 14, 4100 (1975), benzene. [e] Reference 4, piperidine–toluene. [f] Reference 5, methylene chloride. [g] E. Antonini and M. Brunori, "Hemoglobin and Myoglobin in Their Reactions with Ligands", North Holland, Amsterdam, 1971, aqueous solution ethyl isocyanide. [h] Unpublished results, piperidine. [i] At 25 °C unless stated otherwise. [j] Obtained by extrapolation from data at higher temperatures.

Table V. CO and NC Stretching Frequencies of the Heme Models

	ν_{C-O}, cm^{-1}				ν_{N-C}, cm^{-1}				
	CH_3Im	py	CH_3CN	H_2O	CH_3Im	py	pip	CH_3CN	BzNC
$Fe(DMGH)_2$[a]	1978	1985			2141	2145			2167
$Fe(DPGH)_2$[b]		1996							
Fe(TIM)[c]			2030		2181	2184		2189	2189
Fe(TAAB)				2038	2181	2180		2194	2185
FePc[d]	1995	1995			~2160				2180
Fe(PPIX)[e]	1970–1980								
Fe(TPP)[d]							2149		

[a] Reference 7. [b] Reference 6. [c] References 14 and 15. [d] Unpublished results. [e] J. H. Wang, A. Nakahara, and E. B. Fleischer, *J. Am. Chem. Soc.*, 80, 1109 (1958).

glyoximes are clearly the most inert. A similar order with respect to BzNC lability is observed except the phthalocyanine system is now considerably more inert than the porphyrins and is comparable to the TAAB system.

Explanations for the differences in the porphyrins, phthalocyanine, and glyoxime systems have been given previously.[1-4,7] In view of the enormous number of differences in the structure and electronic features of TAAB (hole size, puckering, σ-donor and π-acceptor strength, charge, etc.) and those of the other systems any attempt to attribute specific differences in the axial ligation properties to any particular features is difficult at this stage. These features may become clearer when data are available for other synthetic macrocycles involving more systematic changes in structure.[10] Data for one such system (FeTIM) are reported in a subsequent paper.[17]

Several generalizations emerge from these studies of tetragonal low-spin Fe(II) complexes containing a planar tetradentate ligand, i.e., FeN_4L_2. For a diverse set of in-plane ligands including porphyrin, phthalocyanine, diglyoxime, and TAAB a tremendous variation in kinetic and thermodynamic properties with respect to the axial ligation of imidazole, pyridine, CO, and BzlNC is possible. The following properties are common to all systems: (1) axial substitution reactions proceed via a dissociative mechanism; (2) complexes containing CO and BzlNC are photochromic in the presence of excess amine ligand;[2,18] (3) π-acceptor ligands are more inert trans to methylimidazole than trans to pyridine; (4) nitrogen donors bind according to their pK_b, CH_3CN < py < CH_3Im; (5) nitrogen donors trans to BzlNC are typically much more inert than when trans to the same nitrogen donor in the DMGH and TAAB systems but peculiarly the opposite in the phthalocyanine systems.[19]

Acknowledgment. Support of this research from the National Research Council of Canada and from the Research Corporation is gratefully acknowledged.

Registry No. Fe(TAAB)$FeCl_4$, 62571-26-0; Fe(TAAB)-$(CH_3Im)_2(PF_6)_2$, 63251-23-0; Fe(TAAB)$(py)_2(PF_6)_2$, 63251-24-1; Fe(TAAB)$(CH_3CN)_2(PF_6)_2$, 63251-25-2; Fe(TAAB)(CH_3CN)-(BzlNC)$(PF_6)_2$, 63251-27-4; Fe(TAAB)(CH_3Im)(BzlNC)$(PF_6)_2$, 63251-29-6; Fe(TAAB)(py)(BzlNC)$(PF_6)_2$, 63284-63-9; Fe-(TAAB)$(BzlNC)_2(PF_6)_2$, 63284-65-1; Fe(TAAB)$(CH_3Im)(CO)^{2+}$, 63301-44-0; Fe(TAAB)$(py)(CO)^{2+}$, 63251-30-9; Fe(TAAB)-$(CH_3CN)(CO)^{2+}$, 63251-31-0; Fe(TAAB)$(H_2O)(BzlNC)^{2+}$, 63251-32-1; *o*-aminobenzaldehyde, 529-23-7.

References and Notes

(1) D. V. Stynes and B. R. James, *J. Am. Chem. Soc.*, **96**, 2733 (1974).
(2) D. V. Stynes, *J. Am. Chem. Soc.*, **96**, 5942 (1974).
(3) D. V. Stynes, *Inorg. Chem.*, **16**, 1170 (1977).
(4) D. V. Stynes and B. R. James, *J. Chem. Soc., Chem. Commun.*, 325 (1973).
(5) C. J. Weschler, D. L. Anderson, and F. Basolo, *J. Am. Chem. Soc.*, **97**, 6707 (1975).
(6) L. Vaska and T. Yamaji, *J. Am. Chem. Soc.*, **93**, 6673 (1971).
(7) I. W. Pang and D. V. Stynes, *Inorg. Chem.*, **16**, 590 (1977).
(8) G. A. Melson and D. H. Busch, *J. Am. Chem. Soc.*, **88**, 4834 (1964).
(9) D. H. Busch et al., *Adv. Chem. Ser.*, **No. 100** (1971).
(10) J. C. Dabrowiak, P. H. Merrell, J. A. Stone, and D. H. Busch, *J. Am. Chem. Soc.*, **95**, 6613 (1973).
(11) S. W. Hawkinson and E. B. Fleischer, *Inorg. Chem.*, **8**, 2402 (1969).
(12) I. Ugi and R. Meyer, *Chem. Ber.*, **93**, 239 (1960).
(13) W. J. Geary, *Coord. Chem. Rev.*, **7**, 81 (1971).
(14) D. Baldwin, R. M. Pfeiffer, D. W. Reichgott, and N. J. Rose, *J. Am. Chem. Soc.*, **95**, 5152 (1973).

(15) K. Singh and D. V. Stynes, to be submitted for publication.
(16) The symbolism k_{+x} for addition of x to the five-coordinate intermediate and k_{-x} for dissociation of x from the six-coordinate complexes is used here in place of the more general but less descriptive than k_1, k_2, k_{-1}, and k_{-2} used previously.
(17) E. Wilhelm and R. Battino, *Chem. Rev.*, 73, 1 (1973).
(18) Details of the photochromic properties of these systems will be published elsewhere.
(19) I. W. Pang, K. Singh, and D. V. Stynes, *J. Chem. Soc., Chem. Commun.*, 132 (1976).

Contribution from the Department of Inorganic Chemistry, University of Melbourne, Parkville, Victoria 3052, Australia, and the Department of Chemistry, University of Otago, Dunedin, New Zealand

Paramagnetic Organometallic Molecules. 4.[1] Electrochemical Investigation of the Iron Group Carbonyls and Their Phosphine-Substituted Derivatives

ALAN M. BOND,[2] PETER A. DAWSON, BARRIE M. PEAKE, BRIAN H. ROBINSON, and JIM SIMPSON*

Received November 2, 1976 AIC60786J

The redox behavior of the iron carbonyl species $Fe_3(CO)_{12-n}L_n$ (n = 0–3) and $Fe(CO)_{5-n}L_n$ (n = 0–2) (L = PPh_3, $P(OMe)_3$, $P(OPh)_3$) has been studied in acetone and dichloromethane using the techniques of dc polarography at mercury electrodes and dc cyclic voltammetry at platinum electrodes. A chemically reversible one-electron reduction step was observed for the triiron species within the temperature range 203–293 K. The $E^r_{1/2}$ values for the reduction became increasingly negative with increasing phosphine substitution which correlates well with the charge density on the iron atoms in the parent complexes. The carbonyls $Ru_3(CO)_{12}$ and $Os_3(CO)_{12}$ undergo an irreversible reduction within the temperature range of this investigation leading to rapid decomposition of the carbonyl moieties. Further reduction to the dianions $Fe_3(CO)_{12-n}L_n^{2-}$ occurred for the iron species and caused irreversible disintegration of the cluster unit. A one-electron oxidation step was observed for $Fe_3(CO)_9[P(OMe)_3]_3$. The mononuclear iron derivatives gave well-defined one-electron oxidation and two-electron reduction waves at mercury electrodes. The oxidation step was found to be chemically reversible. No evidence was found for the formation of the radical anion $Fe(CO)_5^{-\cdot}$ under the experimental conditions employed.

Introduction

Earlier papers in this series[3] described an investigation of the remarkably stable paramagnetic radical anions produced from the methinyltricobalt enneacarbonyls $YCCo_3(CO)_9$ and the somewhat less stable phosphine-substituted anions.[4] Electrochemical[3a] and spectral studies[3b] allowed a complete characterization of the redox behavior and provided kinetic and thermodynamic data for the cluster/radical anion couple. These studies also added to our understanding of the HOMO and LUMO levels in the neutral tricobalt carbon cluster and the kinetic and thermodynamic stability of the radical anions was attributed[3b] to an "electron-reservoir" mode of bonding and stereochemical protection afforded by the equatorial and axial carbonyl groups.[5] Whether these ideas have any validity when applied to metal–carbonyl clusters that do not include a nonmetal atom as an integral part of the cluster framework is open to question and thus we extended our investigations to tri- and tetrametallic cluster derivatives.

Trinuclear metal carbonyl clusters $M_3(CO)_{12}$ differ markedly in structure and properties[6] from the tricobalt carbon system but preliminary ESR studies[7] of the products from alkali metal reduction suggested that they might also be reduced to give radical anions. Unambiguous interpretation of the ESR data proved more difficult in this instance and the success achieved with electrochemical studies in the cobalt system[3a] prompted the electrochemical investigation of $M_3(CO)_{12}$ (M = Fe, Ru, Os) and the Lewis base substituted derivatives $Fe_3(CO)_{12-n}L_n$ (n = 0–3) reported herein. Further, since alkali metal reduction apparently produced monomeric and dimeric compounds, as well as trinuclear anions,[8] an electrochemical investigation of $Fe(CO)_5$ and the substituted derivatives $Fe(CO)_{5-n}L_n$ (n = 1, 2) was also undertaken. The electrochemistry of a limited range of iron carbonyl derivatives has been reported previously,[9-14] but this did not include a systematic examination of the redox behavior as the σ-donor and π-acceptor properties of the ligands are varied. Dessy et al.[9] found a reduction wave for $Fe(CO)_5$ at mercury in dimethoxyethane which they interpret as being due to the formation of the unstable radical species $Fe(CO)_5^{-\cdot}$. Picket and Pletcher[13] also described a one-electron reduction of $Fe(CO)_5$ at platinum in THF which they attribute to the overall process

$$Fe(CO)_5 + e^- = {}^1/_2[Fe_2(CO)_8]^{2-} + CO$$

* To whom correspondence should be addressed at the University of Otago.

Experimental Section

$Fe(CO)_5$, $Fe_3(CO)_{12}$, $Ru_3(CO)_{12}$, and $Os_3(CO)_{12}$ were purified by distillation or sublimation in vacuo. Phosphine and phosphite derivatives were prepared from $Fe_3(CO)_{12}$ in hexane by published procedures.[15-18] Separation of the complexes from a particular reaction was most satisfactorily achieved using preparative TLC. The compounds $[Et_3NH][Fe_3(CO)_{11}H]$ and $[(Ph_3P)_2N][HFe(CO)_4]$ were prepared from $Fe(CO)_5$ using procedures based on the methods of McFarlane and Wilkinson[19] and Case and Whiting,[20] respectively.

Electrochemical Instrumentation. Dc polarograms, from which data in this paper are reported, were recorded with a PAR Electrochemistry System, Model 170. Acetone or dichloromethane was used as the solvent with $Et_4N^+ClO_4^-$ as the supporting electrolyte at a concentration of 0.10 (acetone) or 0.08 mol dm^{-3} (dichloromethane). All the solutions were thermostated at the appropriate temperature and degassed with argon for 10 min prior to undertaking measurements. A three-electrode system coupled with positive feedback circuitry was employed to minimize iR drop losses. The working electrode was either a dropping mercury electrode (controlled drop time) or a platinum-disk electrode. The reference electrode was Ag/AgCl [0.1 mol dm^{-3} LiCl (acetone)] and the third electrode was platinum wire. Modifications to the Model 170 Electrochemistry System enabling ac cyclic voltammetry etc. to be performed are described in the literature.[21-23]

Results

$Fe_3(CO)_{12}$. Figure 1 shows the dc polarographic behavior of $Fe_3(CO)_{12}$ in acetone. Two extremely well-defined reduction waves are observed in freshly prepared solutions, with $E_{1/2}$ values −0.21 and −0.76 V vs. Ag/AgCl, respectively. On standing in the electrochemical cell, some decomposition occurred and additional waves appeared near the anodic limit (+0.8 V vs. Ag/AgCl) and at potentials more negative than −1.2 V vs. Ag/AgCl. Little decomposition was observed in dichloromethane and, in this solvent, two well-defined waves were again found ($E_{1/2}$ = −0.30 and −0.64 V vs. Ag/AgCl) corresponding to the same electrode processes as seen in acetone. Analysis of the wave shapes and positions (Tables I and II) and the number of electrons, n, obtained from the limiting-current magnitude and applied potential, were consistent with an initial one-electron reduction followed by